Localized and Dispersive Electronic States at Ordered FePc and CoPc Chains on Au(110)

ARTICLE *in* THE JOURNAL OF PHYSICAL CHEMISTRY C · NOVEMBER 2010

Impact Factor: 4.77 · DOI: 10.1021/jp108734u

8 AUTHORS, INCLUDING:

Maria Grazia Betti
Sapienza University of Rome
159 PUBLICATIONS **1,966** CITATIONS
SEE PROFILE

Roberto Biagi
Università degli Studi di Modena e Reggio …
58 PUBLICATIONS **1,282** CITATIONS
SEE PROFILE

Albano Cossaro
Italian National Research Council
75 PUBLICATIONS **1,553** CITATIONS
SEE PROFILE

Carlo Mariani
Sapienza University of Rome
181 PUBLICATIONS **2,316** CITATIONS
SEE PROFILE

Localized and Dispersive Electronic States at Ordered FePc and CoPc Chains on Au(110)

Maria Grazia Betti,*,† Pierluigi Gargiani,† Riccardo Frisenda,† Roberto Biagi,‡ Albano Cossaro,§ Alberto Verdini,§ Luca Floreano,§ and Carlo Mariani†

Dipartimento di Fisica, Università di Roma "La Sapienza", Piazzale A. Moro 5, I-00185 Roma, Italy, Dipartimento di Fisica, Università di Modena e Reggio Emilia, Via G. Campi 213/A, I-41100 Modena, Italy, and CNR-IOM, Laboratorio Nazionale TASC, Basovizza SS-14, Km 163.5, I-34012 Trieste, Italy

Received: September 13, 2010; Revised Manuscript Received: October 19, 2010

Iron and cobalt phthalocyanines assemble on the Au(110) surface lying parallel to the surface, as deduced by near-edge X-ray absorption fine structure (NEXAFS) taken with linearly polarized radiation at the C and N K edges. The molecular chains, firmly anchored to the underlying metal surface, arrange into long-range ordered rows with a (5×3) symmetry along the [001] azimuthal direction at completion of the first single layer. The interaction process is mainly determined by the d orbitals associated with the central Fe and Co atoms, as observed by valence band photoemission and NEXAFS at the Fe and Co $L_{2,3}$ edges. The spin and orbital configuration of the FePc and CoPc molecules is strongly influenced by the interface with a charge transfer from the underlying metal to the out-of-plane empty states located at the Fe and Co centers of the molecules. This interaction process induces electronic states located at the interface, localized on the central metal atoms and close to the Fermi level (0.2 eV binding energy for FePc and 0.7 eV for CoPc) without energy dispersion, as deduced by angular-resolved photoemission. On the contrary, a delocalized state has been observed with dispersion along the molecular chains, mainly due to the overlapping of the π charge of the macrocycles ligands mediated by the Au substrate.

Introduction

Molecular self-assembly at surfaces is a convenient process for tailoring the functions of organic nanostructures by controlling the properties of the individual molecular building blocks. Molecular building blocks can be combined into desired functional architectures at suitable templates. This variety of molecular superstructures displays a rich selection of intriguing functional properties, which one may exploit in magnetic, optical, and electronic devices.[1,2] The actual feasibility of these construction strategies has already been demonstrated for several applications ranging from spintronics[3] to molecular recognition[4] and from biomimetic applications[5] to catalysis.[4]

Regular patterns of metallorganic molecules at surfaces can ensure formation of a regular grid of metal atoms surrounded by macrocycle ligands, allowing for tunable anchoring sites, molecular orientation, and interaction strength. Organometallic molecules like metal−phthalocyanines ($M-C_{32}H_{16}N_8$, MPc) are archetypal metallorganic complexes constituted by four pyrrolic and four benzene rings arranged around the central metal atom. These stable aromatic dyes have a 2-fold interest: the π conjugation guarantees charge delocalization and electron mobility, and the central metal atom plays a crucial role to determine the electronic/magnetic properties.[1,2] Furthermore, the unique flexibility of MPcs in coordinating more than 70 elemental ions and the tendency to self-assemble on metal surfaces forming ordered aggregates or films make MPcs suitable systems to control and manipulate the electronic and magnetic properties of desired organic nanostructures at surfaces.

The final aim is controlling the functions of these ordered molecular structures and the degree of charge delocalization. This goal is strictly related to the control of the interaction strength of the macrocycles and of the central metal atoms with the underlying substrate.[6−10] If the charge located on the macrocycles and/or on the central metal atoms is delocalized, it should be revealed by an electronic band dispersion. Generally, π-conjugated molecules deposited on metal substrates adsorb in a planar configuration, so far only limited experimental results have been collected on the intermolecular dispersion of electronic states of molecular single layers[11−15] or multilayers.[16−19] In particular, copper−phthalocyanine deposited on the Au(110) surface forms ordered chains along the Au reconstructed channels, giving rise to a delocalized quasi-1D band dispersive along the chains,[12] probably due the overlapping of the macrocycle states mediated by the gold substrate. Our purpose is to identify the origin and nature of the electron states located at the interface for the ordered FePc and CoPc molecular structures deposited on the Au(110) surface, to control the role of the macrocycle ligands and the central metal atoms in the interaction process, and to verify the degree of delocalization by controlling the band dispersion.

Experimental Section

Photoemission experiments have been carried out at the surface physics laboratory LOTUS at the Universita "La Sapienza" in Roma; NEXAFS experiments have been performed at the ALOISA beamline of the Elettra synchrotron radiation facility, in ultrahigh-vacuum (UHV) systems with base pressures better than 1×10^{-10} mbar. Both laboratories are equipped with analogous ancillary facilities for sample preparation and molecular deposition and control. Surface quality and cleanness were checked by means of low-energy electron-diffraction

* To whom correspondence should be addressed. E-mail: maria.grazia.betti@roma1.infn.it.
† Università di Roma "La Sapienza".
‡ Università di Modena e Reggio Emilia.
§ Laboratorio Nazionale TASC.

10.1021/jp108734u
Published on Web 11/16/2010

(LEED), reflection high-energy electron-diffraction (RHEED), and core-level photoemission spectroscopy.

The NEXAFS spectra were obtained in the partial electron yield mode by means of a channeltron facing the sample. The photon energy was spanned in the 282−300, 396−412, 704−732, and 773−802 eV energy ranges for the C K and N K edges, Fe $L_{2,3}$ edges, and Co $L_{2,3}$ edges, respectively. In order to reduce the NEXAFS background originated by the secondary electrons and by the Au 4f photoelectrons, a grid in front of the channeltron was negatively polarized to −230, −360, −680, and −760 V for the C, N, Fe, and Co thresholds, respectively. Absolute calibration of the photon energy was obtained for the C, N, and Fe thresholds thanks to the simultaneous acquisition of the drain current on the metal-coated surface of the last beamline mirror, which displays residual traces from the aforementioned three elements. C and N have been calibrated by real-time acquisition of the gas-phase absorption spectra (from CO_2 and N_2) in the ALOISA in-line windowless ionization cell.[20] The Co threshold has been calibrated by taking photoemission spectra with the experimentally determined value of the spectrometer work function.

The NEXAFS spectra were collected in the two opposite orientations of the scattering plane with respect to the electric field of the linearly polarized X-ray beam, namely, transverse magnetic (TM) and transverse electric (TE) polarization. The polarization condition was changed by rotating the surface around the X-ray axis while keeping a costant grazing incidence of 6°; thus, TE polarization corresponds to the electric field oriented in the surface plane, while TM corresponds to an almost normal orientation of the electric field. Data have been taken with the sample kept at 150 K to minimize the radiation damage.

The HR-ARUPS spectra have been excited with a He discharge source (He Iα photons, $h\nu = 21.218$ eV). The photoemitted electrons were analyzed in the plane of incidence, with a high-resolution Scienta SES-200 hemispherical analyzer, by using a two-dimensional multichannel-plate detector. Angular resolved spectra were analyzed in the plane of incidence; the angular and intrinsic energy resolutions are 0.18° and 16 meV, respectively.

The Au(110) surface has been cleaned by double-step sputtering−annealing treatment (Ar^+ ions at 1000 eV, $T = 725$ K, followed by 500 eV, 530 K). FePc and CoPc were evaporated from a resistively heated quartz crucible at a low deposition rate (few Å/min) estimated by means of a quartz microbalance to maintain good vacuum conditions and smooth film growth. FePc and CoPc nominal thickness is referred to an equivalent uniform bulklike layer with a density of about 1.6 g/cm^3. MPc deposition on the surface has been done keeping the Au(110) substrate at 430 K to improve the long-range order of the single layer. Subsequent deposition to achieve the few nanometer thick thin films (TF) was performed maintaining the substrate at room temperature (RT). A single layer (SL) is defined herewith as an ordered layer of molecules laying down and covering the whole Au(110) surface, corresponding to about 4 Å of nominal uniform coverage.

Both FePc and CoPc present analogous adsorption evolution from the well-ordered SL to thin-film formation. Molecules deposited on the (1 × 2)-reconstructed Au(110) surface induce a (5 × 5) periodicity at the sub-SL stage and then a (5 × 3) reconstruction at completion of the SL, in agreement with previous observations on a series of MPc molecules prepared on the same substrate.[10,12] As exemplary evolution, in Figure 1 we show the sharp long-range ordered RHEED reconstruction patterns for the FePc adsorption on Au(110), taken along the [001] azimuthal direction during MPc growth. There is a clear evolution from the 2-fold symmetry of the clean substrate to the subsequent 5-fold and 3-fold symmetries observed for the SL. The (5 × 3) reconstruction has been previously justified by formation of long-range ordered molecular chains arranged along the underlying reconstructed Au channels.[10,21] We did not observe any electron beam-induced damage during the RHEED experiment.

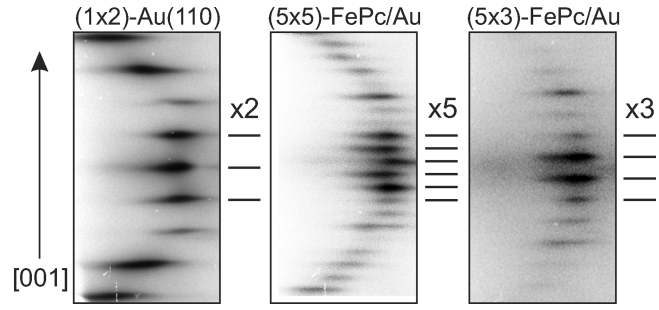

Figure 1. RHEED patterns along the [001] azimuthal direction as a function of FePc coverage at the SL stage. Clean Au(110) (1 × 2)-reconstructed surface (left), (5 × 5) (center), and (5 × 3) (right) FePc/Au(110) SL.

Results and Discussion

Our first aim is to assess the orientation of the FePc and CoPc molecules on the Au(110) surface and whether they stay intact when adsorbed on the surface. Carbon and nitrogen K edges and Fe(Co) $L_{2,3}$ absorption edges can give information not only on the molecular orientation of the FePc and CoPc regular patterns at the Au(110) surface; they also allow identifying the role of the regular grid of central metal atoms and of the surrounding macrocycle ligands in the interaction process. At the simplest level of description, the absorption edges of the macrocycle ligands represent the unoccupied orbitals and can be intepreted to assess the molecular orientation and orbitals involved in the interaction process. However, the interpretation of the fine structure of the transition metal edges is more controversial, starting from the pioneering study by Koch et al.[22] In fact, it is not directly related to the unoccupied states, because of the strong influence of atomic multiplet splitting and Coulomb-exchange interaction. Though a simple description cannot fully identify the 3d orbital ground state configuration for the central metal atom, the comparison of the Fe(Co) $L_{2,3}$ edges for a SL and a TF can clarify the evolution of the spin and orbital states.

The NEXAFS C and N K-edge data for the SL and TF of FePc and CoPc grown on the Au(110) surface are shown in Figures 2 and 3, respectively. Both C and N K edges are taken with linearly polarized radiation, with the electric field vector either parallel (TM) or normal (TE) to the scattering plane, i.e., given the experimental geometry sketched in the figures, with the electric field polarization vector correspondingly almost normal or parallel to the crystal surface plane, respectively. The C and N 1s core-level photoemission binding energies (BE) are marked with bars in the top axes of each panel. The NEXAFS data are characterized by multiple absorption peaks, which we detail later, basically associated with transitions from the C 1s and N 1s core levels to the empty states located on the benzene and pyrrole macrocycles of π^* and σ^* character. The comparison of the spectra at the C and N edges reveals the same fine structures for the FePc and CoPc (5 × 3)-recostructed phases. In particular, the main unoccupied level in these molecules is formed by π^* states delocalized mainly on the pyrrole macro-

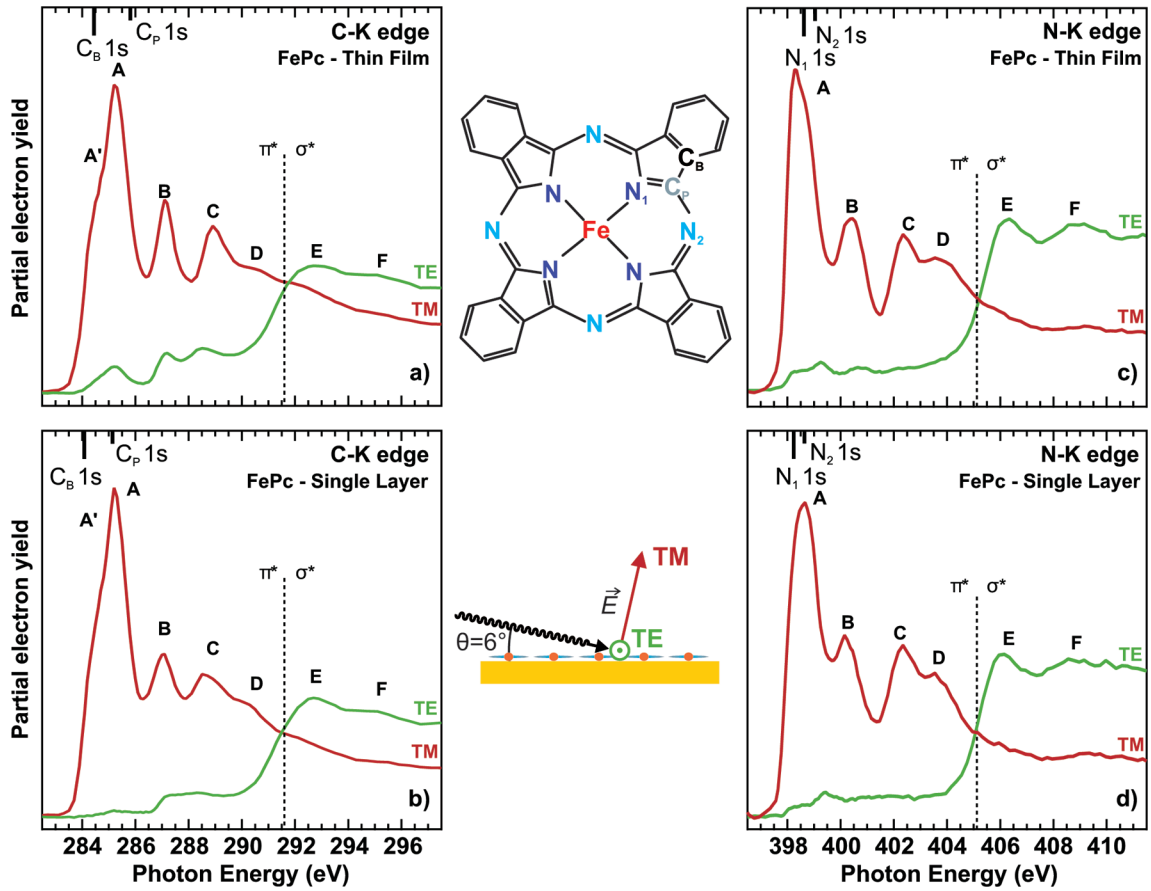

Figure 2. C K-edge NEXAFS data for the FePc/Au(110) system at the TF (a) and SL (b) coverage; N K-edge NEXAFS data for the FePc/Au(110) system at the TF (a) and SL (b) coverage. In all four panels the corresponding core-level BEs (C_B and C_P 1s, N_1-isoindole, and N_2-azamethine 1s) are marked by vertical bars. A sketch of the FePc molecule and the experimental geometry is reported in the central part of the figure.

cycles, thus available for transitions from both the C and the N 1s initial states, justifying the line shape similarity for both edges.

There is a clear dichroic effect at the C and N K edges for the two polarizations at both MPcs and at both the SLs and the TFs, with distinct polarization dependence on the π^* and σ^* resonances. Due to the dipolar character of these states, the observed dichroism constitutes definite evidence of a planar orientation of the FePc and CoPc molecules both at the SL coverage stage and for the few nanometer thick thin films grown on Au(110). The Au(110) surface favors the flat-lying configuration of several aromatic organic molecules at the monolayer stage,[21,23−32] with the molecules arranged along the troughs of the 3-fold reconstructed underlying Au channels.[12,21,31−34] In particular, MPcs with a different central metal atom have been previously observed in the planar configuration on Au surfaces at the SL phase.[6,7,21,30,32,33,35] Thus, the planar configuration achieved in the SL phase is preserved also when FePc and CoPc thin films of a few nanometer thickness are grown on the first flat-lying highly ordered SL on the Au(110) surface, in agreement with previous data for MPc adsorption on the Au(001) surface.[36]

The C and N absorption near-edge fine structures present a similar sequence of features and line shapes. We briefly recall the assignment of the main spectral peaks. The shoulder A′ at the C K edge is due to absorption from the C atoms in the benzene rings (C_B 1s), and A is due to transitions from the C atoms in the pyrrole rings (C_P 1s), while structures B, C, and D are due to transitions to LUMO+n states mainly involving the pyrrole ring with C−N bonds.[32] In the N K-edge data, the absorption features present analogous line shape and sequence as in the C K-edge data, and the main peak A is due to transition from the N 1s state of the two unequivalent N atoms (N_1-isoindole and N_2-azamethine) to the π^* LUMO delocalized on the pyrrole ring.

Despite the very similar line shapes, there are subtle differences in the NEXAFS line shape on going from the SL to the TF phase for both FePc and CoPc on Au(110). There is an energy difference of ≃0.4−0.5 eV between the initial state C_P BE and the corresponding NEXAFS peaks A for the TFs, a sign of an evident excitonic effect. The exciton energy is negligible for the carbon atoms in the benzene ring; in fact, the C_B binding energy is almost equivalent to the A′ absorption energy. This is due to the more delocalized nature of the final state involving the π^* states. An important effect is that the exciton, clearly visible on the pyrrole ring for both FePc and CoPc TFs, is quenched when the molecules form a SL array on Au(110), indicating an electron−hole screening due to the underlying metal electrons. The NEXAFS features in the SLs appear slightly broader than in the corresponding TFs. Despite these differences in exciton effect and line shape, the C and N K signals reveal that the ligand macrocycles in the SLs are slightly affected by the interaction with the Au metallic states, as previously observed for MPcs deposited on metal substrates.[21,32]

The interaction effect on the Fe and Co central metal atoms can be analyzed by studying the absorption from the 2p core levels. The $L_{2,3}$ edges are ideal not only for extracting detailed information on the interaction process but also to study the evolution of the empty states associated with the orbital and spin configuration of the central metal atom of the single layer

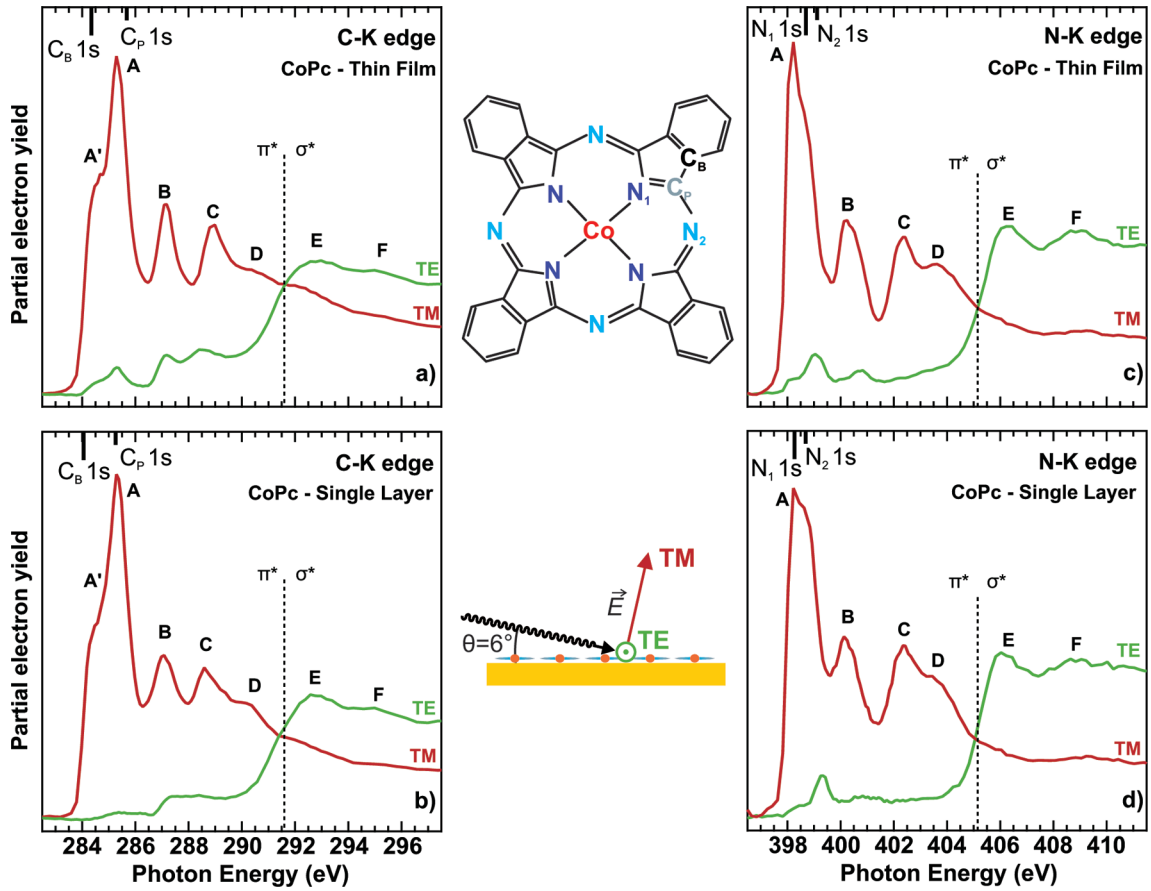

Figure 3. C K-edge NEXAFS data for the CoPc/Au(110) system at the TF (a) and SL (b) coverage; N K-edge NEXAFS data for the CoPc/Au(110) system at the TF (a) and SL (b) coverage. In all four panels the corresponding core-level BEs (C_B and C_P 1s, N_1-isoindole, and N_2-azamethine 1s) are marked by vertical bars. A sketch of the CoPc molecule and of the experimental geometry is reported in the central part of the figure.

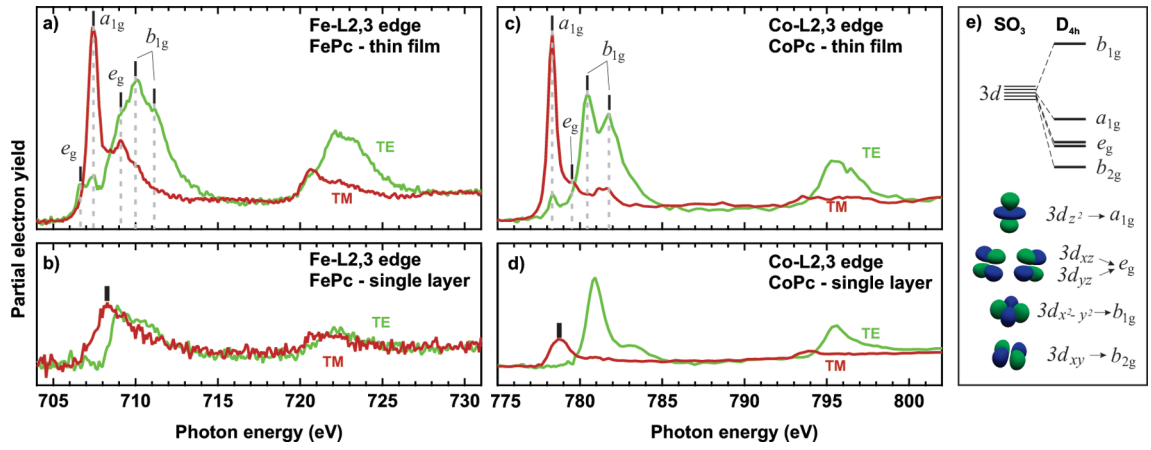

Figure 4. Fe $L_{2,3}$ NEXAFS absorption edge for the TF (a) and SL (b) FePc on Au(110); Co $L_{2,3}$ NEXAFS absorption edge for the TF (c) and SL (d) CoPc on Au(110); (e) schematic sketch of the metal 3d orbital splitting from the SO_3 spherical symmetry to the D_{4h} tetragonal distortion in the MPc molecules. TF orbital assignment according to ref 37.

of FePc and CoPc chains on the Au(110) substrate. We compare the Fe and Co $L_{2,3}$ edges at the SL and TF phases on Au(110), as reported in Figure 4. At first sight, we notice the strong dichroism depending on the light polarization, confirming a definite orientation of the molecules at both thickness, once taken into consideration each specific orbital dipolar orientation, as done below. The present FePc-TF and CoPc-TF data are in agreement with previous Fe $L_{2,3}$ and Co $L_{2,3}$ linearly polarized measurements, where adsorbed FePc and CoPc are flat lying on a thick Au buffer layer on sapphire[37] and on the Au(001) surface,[38] respectively.

It is hard to univocally identify the unoccupied metal d states directly involved in the interaction process. At a first level of interpretation, the five 3d orbitals are split by the ligand field interaction, mostly determined by the symmetry group: we recall that the d-like orbitals of the Fe and Co atoms in the MPc molecule present reduced symmetry with respect the purely atomic spherical symmetry, resulting in three singlets and a doublet labeled according to the D_{4h} irreducible representations (see right panel in Figure 4). The reduced symmetry gives rise to the empty b_{1g} state with $d_{x^2-y^2}$ symmetry, hybridized with the π orbital localized on the nitrogen atoms, while the

occupancy of the a_{1g} state (d_{z^2}) and the doublet e_g (d_{zy}, d_{xz}), mainly localized on the central magnetic atoms is more controversial, as recent theoretical predictions, affected by the use of different exchange-correlation functionals, produce different energy sequence and symmetry mixing.[39−42] A detailed analysis of the fine structure of the $L_{2,3}$ edges requires a theoretical model including atomic multiplet splitting, crystal field effect, and Coulomb-exchange interaction.[43,44] Furthermore, at the SLs, where the interaction causes a symmetry breaking, a one-to-one correspondence of the orbitals can be hidden by the rehybridization process.

The flat-lying orientation of both FePc and CoPc TFs grown on Au(110) discussed above helps in identifying the empty orbitals accessed by excitation of the 2p core-level electrons. Taking into account the sequence of spin-split molecular orbitals assigned in FePc[37] and CoPc[38] and the expected final low spin state ($S = 1$ for FePc and $S = 1/2$ for CoPc),[44,46] we can assign the different absorption contributions, considering the symmetry assessed by electrons excited from the $2p_{3/2}$ or $2p_{1/2}$ initial states on the basis of the proper selection rules. In the TM polarized spectrum, where states localized normal to the molecular plane are accessible, the huge L_3 white line of the FePc-TF at 707.4 eV photon energy is due to the a_{1g} single empty state, while the higher lying structures at 709.1 and 710.1 eV may be mainly attributed to the e_g state of d_{zy} and d_{xz} character.[37] In the TE polarized spectrum for the FePc-TF, the a_{1g} state is strongly reduced, owing to its charge-density localization in the direction perpendicular to the molecular plane. The small structure at the edge at 706.7 eV and the peak at 709.1 eV with a minor dichroic effect were previously attributed to the e_g state.[37] The higher lying peaks at 710.1 and 711.3 eV are due to b_{1g} states[37] with exchange splitting of 1.2 eV (confirmed by the analogous features above the L_2 edge). Within the same interpretation framework of FePc, the very intense CoPc L_3 white line at 778.3 eV (TM polarized spectrum) is assigned to the single empty a_{1g} state,[38] while the e_g state (779.5 eV) is clearly less intense than in FePc, owing to the higher d-state occupancy for the CoPc molecule. The most intense higher lying absorption features (780.5 and 781.8 eV, TE polarized spectrum) can be associated with b_{1g} with dominant $d_{x^2-y^2}$ character. The main spectral differences in the CoPc-TF with respect to FePc are the stronger dichroic effect affecting the higher lying features above the edges and a more intense $I(L_3)/I(L_3 + L_2)$ intensity ratio (0.79 for CoPc, 0.74 for FePc, evaluated for the integrated signals adding the TE and TM polarized spectra), in agreement with the low spin state for both systems, which determines an increasing intensity ratio upon increasing d-state occupancy.[43−45]

We observe an $L_{2,3}$ line shape evolution comparing the TF absorption features to the SL ones. There is still dichroism associated with the molecular orientation, but the spectral features are strongly influenced by the interaction process. In particular, the a_{1g} state with d_{z^2} symmetry is heavily reduced in both FePc and CoPc SLs on Au(110), while a new absorption feature becomes visible at 708.25 (778.77 eV) for the FePc (CoPc) SL for the TM spectrum (marked with a thick tick in Figure 4b and 4d), showing a clear dichroic response, caused by a general redistribution of empty states located in levels out of the molecular plane accessed by the core−electrons. The spectral features excited by photons impinging with TE polarization are less influenced by the interaction process in the FePc SL, although the intensity of the b_{1g} states is reduced. In the CoPc SL, the molecular in-plane metal-derived orbitals seem less involved in the interaction with the underlying metal surface, as the spectral density distribution associated with the b_{1g} levels maintains a consistent intensity above the first absorption peaks. The $L_{2,3}$ line shape modifications directly imply a definite involvement of the out-of-plane orbitals of the central metal atoms interacting with the quasi-free electrons of the underlying metallic substrate, in contrast with the π orbitals of the macrocycles. Finally, the $I(L_3)/I(L_3 + L_2)$ intensity ratio is reduced with respect to the TFs (about −4% for FePc and −10% for CoPc) but maintains a higher value than the statistical atomic-like. This evidence, along with the reduction of the a_{1g} empty state that is mainly responsible for the electronic magnetic moment of the molecule, may indicate a reduction of the magnetic moment of these adsorbed FePc and CoPc SLs. Theoretical models including atomic multiplet structure for this specific SL configuration would be desirable to quantify the contribution of the spin state and of the ligand-field interaction in determining the intensity ratio. A reduction from 2.03 μ_B (free FePc molecule) to 1.05 μ_B has been recently calculated for FePc, when it is adsorbed on the Au(111) surface.[9] In this latter case, a strong reduction of the d_{z^2} orbital upon adsorption has been predicted, while the residual magnetic moment is mainly attributed to residual $d_{xz,yz}$ states. Though the magnetic moment reduction is strictly dependent on the adsorption site and configuration, the conclusions for the FePc molecule adsorbed on the Au(111) surface are consistent with our observation of state redistribution of a reduction of the a_{1g} state for the SL on Au(110). On the other hand, theoretical data with the same ab initio approach for CoPc/Au(111)[47] predict a full quenching of the magnetic moment of the pristine free CoPc molecule (1.09 μ_B) due to orbital mixing causing occupation of the spin-down states. This picture is consistent with our observation of the a_{1g} reduction at the CoPc-SL, with a minor role of the e_g states, and with a rehybridization process involving the in-plane b_{1g} levels. The orbital and spin configurations of the ordered chains of FePc and CoPc deposited on the Au(110) surface definitely indicate a strong interaction of the central metal atoms with the underlying substrate, a rehybridization of the d orbital with a major influence on the d state localized out of the molecular plane. The evolution of the electronic configuration suggests a reduction of the spin magnetic moment, though only a theoretical prediction or specific measurements, like magnetic dichroism, could quantify it.

The experimental evidence that an interaction involves the empty d orbitals of the Fe (Co) central metal atom in establishing the formation of MPc chains along the Au(110) channels at the highly ordered SL stage can be verified by exploring the electronic spectral density of occupied states in the valence band region by means of high-resolution photoemission. The normal-emission HR-UPS spectra for the FePc and CoPc (5 × 3)-SLs on Au(110) are shown in Figures 5 and 6 (left panels), respectively. The Au(110)-(1 × 2) surface states (S_1 and S_2) are quenched upon MPc adsorption, and a sequence of interface states (I_n) emerges at the SL for both MPcs, which we can associate to macrocycle-related interface structures, in full agreement with photoemission data obtained by comparing different MPcs (M = Fe, Co, Ni, Cu, Zn).[10] In the low-BE region, apart from the interface-HOMO of a_{1u} symmetry at 0.95 eV BE in the FePc-SL (1.05 eV in CoPc-SL),[10] a specific interaction state emerges only for FePc and CoPc: the I_0 interface state (localized at 0.21 eV for FePc and 0.73 eV for CoPc) associated with electronic interacting states involving the central metal atom.[10]

The strong white-line reduction at the L_3 absorption edges, attributed to occupation of the a_{1g} levels can be related to the appearance of I_0, thus univocally identifying the metal orbitals

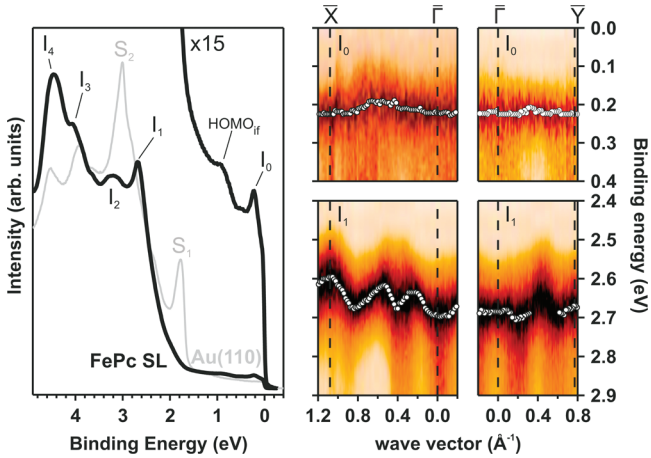

Figure 5. Angular-resolved ultraviolet photoelectron spectroscopy data for the (5 × 3)-FePc/Au(110) single layer. (Left) Data integrated across $\bar{\Gamma}$ for the FePc-SL (black lines) and the clean Au(110) spectrum (gray line). (Right) Energy dispersion of the relevant interface peaks I_0 and I_1 as a function of the parallel wave vector along the $\bar{\Gamma}\bar{X}$ and the $\bar{\Gamma}\bar{Y}$ directions of the (1 × 1) SBZ.

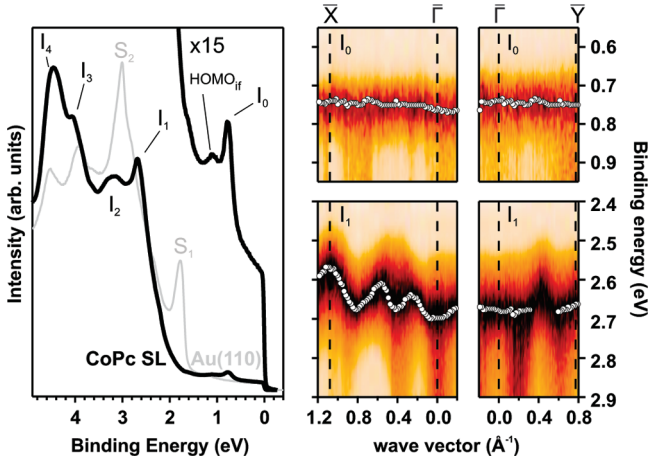

Figure 6. Angular-resolved ultraviolet photoelectron spectroscopy data for the (5 × 3)-CoPc/Au(110) single layer. (Left) Data integrated across $\bar{\Gamma}$ for the CoPc-SL (black lines) and the clean Au(110) spectrum (gray line). (Right) Energy dispersion of the relevant interface peaks I_0 and I_1 as a function of the parallel wave vector along the $\bar{\Gamma}\bar{X}$ and the $\bar{\Gamma}\bar{Y}$ directions of the (1 × 1) SBZ.

involved in the interaction process, completing previous tentative attribution.[10] Although the interaction process can induce a rehybridization involving more states, the main channel of charge transfer may be associated with the single-occupied a_{1g} state hybridized with the underlying Au states for both the CoPc-SL[10,48] and the FePc-SL. The attribution of the main interface states (I_0 and I_n) either to metal-related or to macrocycle-associated levels is corroborated by the HR-ARUPS data taken along the two main symmetry directions of the surface Brillouin zone (SBZ) for the (5 × 3) FePc and CoPc SLs on Au(110), as shown in Figures 5 and 6 (right panels), respectively. The electronic band mapping has been drawn as a function of the parallel momentum $k_{||}$, following the relation $k_{||} = \sqrt{2mE/\hbar}\sin\theta$, along the and $\bar{\Gamma}\bar{X}$ and $\bar{\Gamma}\bar{Y}$ symmetry directions of the (1 × 1) SBZ. I_1 presents exactly the same characteristics for both FePc and CoPc SLs, exhibiting a 90 ± 10 meV energy bandwidth and a 5-fold symmetry with respect to the (1 × 1) SBZ, in perfect agreement with the observed 5-fold symmetry along the $[1\bar{1}0]$ direction and also in agreement with previous observation on the (5 × 3)-CuPc SL/Au(110).[12] A hardly discernible dispersion within the experimental error is instead present along the $\bar{\Gamma}\bar{Y}$ direction. The 5-fold dispersion matches the structural 5-fold symmetry of the flat-lying MPc molecules arranged into ordered chains.[10] The absence of relevant line shape changes in the C and N K edges for the SLs suggests that the delocalization is mainly associated with macrocycle orbitals overlapping along the chains, probably mediated by the underlying Au substrate. Recently, delocalized states[15] along ordered pentacene chains[49] have been observed, associated with charge delocalization along the molecular chains, mediated by metal−molecular state intermixing.[50,51] A two-dimensional electronic state dispersion has been measured for other ordered structures built up by aromatic oligomer (PTCDA) deposited on the Ag(111) surface.[11] Due to all this evidence, we can definitely associate the I_1 level to an overlapping interacting Fe(Co)*Pc*-macrocycle state along the molecular chains mediated by the underlying Au metallic states.

While the macrocycle-associated peak I_1 presents an energy dispersion following the expected 5-fold symmetry along the molecular chains, the metal-related interface state I_0 is localized, as reflected by the absence of energy dispersion along the high-symmetry directions of the SBZ. The localized character constitutes a further confirmation of the origin of this metal-related electronic state, mainly associated with intermixing of the d_{z^2} Fe and Co out-of-plane states, with the underlying Au electrons. This localized level associated with the d states also ensures firm anchoring of the molecules on the Au(110) substrate, producing the observed density of empty states remodulation at the SL level. Although a site-specific dependence of the molecule−substrate interaction is expected, first-principles theoretical predictions for MPc adsorption on Au(111) observe a high d-related density of states close to the Fermi level for FePc[9] and at higher binding energy for CoPc,[47] in agreement with our assignment. This agreement suggests an interaction mainly driven by the localized out-of-plane d orbital of the central metal atom with the underlying delocalized metallic states.

Conclusions

Metal phthalocyanines are ideal organometallic systems to control the degree of charge delocalization at hybrid organic/metal interfaces and to tune the electronic properties with the appropriate choice of the coordinated central metal atoms. In fact, FePc and CoPc form highly long-range ordered molecular chains, lying flat along the Au(110) reconstructed channels, as brought to light through the dichroic NEXAFS signal at the C and N K edges. The electronic charge is delocalized along the chains because of the overlapping π-conjugated electronic states located on the benzene and pyrrole macrocycles, giving rise to dispersive states with a ×5 periodicity, reflecting the molecular arrangement along the chains. The spin and orbital configuration of the central metal atoms is strictly related to the strength of the interaction process. The firm anchoring of the CoPc and FePc molecules with the underlying metal substrate is determined by the interaction of the d-orbital states with the underlying metal. The evolution of the out-of-plane d orbital upon the molecular adsorption, as investigated by NEXAFS at the $L_{2,3}$ edges and valence band photoemission, suggests a reduction of the spin magnetic moment. The rehybridization process is accompanied by a charge donation from the underlying metal, giving rise to highly localized induced electronic states located at the central metal atom sites.

Acknowledgment. We thank the Elettra national facility of synchrotron radiation, the Sapienza Università di Roma, and the PRIN project of MIUR for support.

References and Notes

(1) Forrest, S. R. *Nature* **2004**, *428*, 911–8.
(2) Karl, N. In *Organic electronics: science and applications*; Agranovich, V. M. Ed.; IOS: Amsterdam, 2002.
(3) Fert, A. *Rev. Mod. Phys.* **2008**, *80*, 1517–1530.
(4) Leznoff, C. C.; Lever, A. B. P. *Phthalocyanines: properties and applications*; Wiley-VCH: Weinheim, 1989.
(5) Grennberg, H.; Faizon, S.; Bäckvall, J.-E. *Angew. Chem., Int. Ed. Engl.* **1993**, *32*, 263–264.
(6) Lu, X.; Hipps, K. W. *J. Phys. Chem. B* **1997**, *101*, 5391–5396.
(7) Lu, X.; Hipps, K. W.; Wang, X. D.; Mazur, U. *J. Am. Chem. Soc.* **1996**, *118*, 7197–7202.
(8) Ruocco, A.; Evangelista, F.; Attili, A.; Donzello, M. P.; Betti, M. G.; Giovanelli, L.; Gotter, R. *J. Electron Spectrosc. Relat. Phenom.* **2004**, *137*−*140*, 165–169.
(9) Hu, Z.; Li, B.; Zhao, A.; Yang, J.; Hou, J. G. *J. Phys. Chem. C* **2008**, *112*, 13650–13655.
(10) Gargiani, P.; Angelucci, M.; Mariani, C.; Betti, M. G. *Phys. Rev. B* **2010**, *81*, 085412.
(11) Temirov, R.; Soubatch, S.; Luican, A.; Tautz, F. S. *Nature* **2006**, *444*, 350–3.
(12) Evangelista, F.; Ruocco, A.; Gotter, R.; Cossaro, A.; Floreano, L.; Morgante, A.; Crispoldi, F.; Betti, M. G.; Mariani, C. *J. Chem. Phys.* **2009**, *131*, 174710.
(13) Toyoda, K.; Hamada, I.; Yanagisawa, S.; Morikawa, Y. *Appl. Phys. Express* **2010**, *3*, 025701.
(14) Chen, L.; Li, H.; Wee, A. T. S. *Nano Lett.* **2009**, *9*, 4292–6.
(15) Annese, E.; Fujii, J.; Baldacchini, C.; Zhou, B.; Viol, C.; Vobornik, I.; Betti, M. G.; Rossi, G. *Phys. Rev. B* **2008**, *77*, 1–5.
(16) Annese, E.; Viol, C. E.; Zhou, B.; Fujii, J.; Vobornik, I.; Baldacchini, C.; Betti, M. G.; Rossi, G. *Surf. Sci.* **2007**, *601*, 4242–42455.
(17) Hasegawa, S.; Mori, T.; Imaeda, K.; Tanaka, S.; Yamashita, Y.; Inokuchi, H.; Fujimoto, H.; Seki, K.; Ueno, N. *J. Chem. Phys.* **1994**, *100*, 6969.
(18) Yamane, H.; Kera, S.; Okudaira, K.; Yoshimura, D.; Seki, K.; Ueno, N. *Phys. Rev. B* **2003**, *68*, 1–4.
(19) Koch, N.; Vollmer, a.; Salzmann, I.; Nickel, B.; Weiss, H.; Rabe, J. *Phys. Rev. Lett.* **2006**, *96*, 10–13.
(20) Floreano, L.; Naletto, G.; Cvetko, D.; Gotter, R.; Malvezzi, M.; Marassi, L.; Morgante, A.; Santaniello, A.; Verdini, A.; Tommasini, F.; Tondello, G. *Rev. Sci. Instrum.* **1999**, *70*, 3855.
(21) Floreano, L.; Cossaro, A.; Gotter, R.; Verdini, A.; Bavdek, G.; Evangelista, F.; Ruocco, A.; Morgante, A.; Cvetko, D. *J. Phys. Chem. C* **2008**, *112*, 10794–10802.
(22) Koch, E.; Jugnet, Y.; Himpsel, F. *Chem. Phys. Lett.* **1985**, *116*, 7–11.
(23) Bavdek, G.; Cossaro, A.; Cvetko, D.; Africh, C.; Blasetti, C.; Esch, F.; Morgante, A.; Floreano, L. *Langmuir* **2008**, *24*, 767–72.
(24) Vilmercati, P.; Cvetko, D.; Cossaro, A.; Morgante, A. *Surf. Sci.* **2009**, *603*, 1542–1556.
(25) Gador, D. *J. Electron Spectrosc. Relat. Phenom.* **1998**, *96*, 11–17.
(26) Stadler, C.; Hansen, S.; Pollinger, F.; Kumpf, C.; Umbach, E.; Lee, T.-L.; Zegenhagen, J. *Phys. Rev. B* **2006**, *74*, 035404.
(27) Betti, M. G.; Kanjilal, A.; Mariani, C. *J. Phys. Chem. A* **2007**, *111*, 12454–7.
(28) Chiodi, M.; Gavioli, L.; Beccari, M.; Di Castro, V.; Cossaro, A.; Floreano, L.; Morgante, A.; Kanjilal, A.; Mariani, C.; Betti, M. *Phys. Rev. B* **2008**, *77*, 115321.
(29) Evangelista, F.; Ruocco, A.; Pasca, D.; Baldacchini, C.; Betti, M.; Corradini, V.; Mariani, C. *Surf. Sci.* **2004**, *566*−*568*, 79–83.
(30) Corradini, V.; Menozzi, C.; Cavallini, M.; Biscarini, F.; Betti, M. G.; Mariani, C. *Surf. Sci.* **2003**, *532*−*535*, 249–254.
(31) Prato, S.; Floreano, L.; Cvetko, D.; Renzi, V. D.; Morgante, A.; Modesti, S.; Biscarini, F.; Zamboni, R.; Taliani, C. *J. Phys. Chem. B* **1999**, *103*, 7788–7795.
(32) Calabrese, A.; Floreano, L.; Verdini, A.; Mariani, C.; Betti, M. G. *Phys. Rev. B* **2009**, *79*, 115446.
(33) Cossaro, A.; Cvetko, D.; Bavdek, G.; Floreano, L.; Gotter, R.; Morgante, A.; Evangelista, F.; Ruocco, A. *J. Phys. Chem. B* **2004**, *108*, 14671–14676.
(34) Buongiorno Nardelli, M.; Cvetko, D.; De Renzi, V.; Floreano, L.; Gotter, R.; Morgante, A.; Peloi, M.; Tommasini, F.; Danieli, R.; Rossini, S.; Taliani, C.; Zamboni, R. *Phys. Rev. B* **1996**, *53*, 1095–1098.
(35) Takami, T.; Carrizales, C.; Hipps, K. *Surf. Sci.* **2009**, *603*, 3201–3204.
(36) Molodtsova, O. V.; Knupfer, M.; Ossipyan, Y. A.; Aristov, V. Y. *J. Appl. Phys.* **2008**, *104*, 083704.
(37) Bartolomé, J.; Bartolomé, F.; García, L. M.; Filoti, G.; Gredig, T.; Colesniuc, C. N.; Schuller, I. K.; Cezar, J. C. *Phys. Rev. B* **2010**, *81*, 195405.
(38) Kroll, T.; Aristov, V. Y.; Molodtsova, O. V.; Ossipyan, Y. A.; Vyalikh, D. V.; Büchner, B.; Knupfer, M. *J. Phys. Chem. A* **2009**, *113*, 8917–22.
(39) Calzolari, A.; Ferretti, A.; Nardelli, M. B. *Nanotechnology* **2007**, *18*, 424013.
(40) Marom, N.; Kronik, L. *Appl. Phys. A: Mater. Sci. Process.* **2009**, *95*, 159–163.
(41) Marom, N.; Kronik, L. *Appl. Phys. A: Mater. Sci. Process.* **2009**, *95*, 165–172.
(42) Kuźmin, M.; Hayn, R.; Oison, V. *Phys. Rev. B* **1991**, *44*, 12424–12439.
(43) Thole, B.; van Der Laan, G. *Phys. Rev. B* **1991**, *44*, 12424–12439.
(44) Thole, B.; Van Der Laan, G.; Butler, P. *Chem. Phys. Lett.* **1988**, *149*, 295–299.
(45) Ksohino, M.; Kurata, H.; Isoda, S.; Kobayashi, T. *Micron* **2000**, *31*, 373–380.
(46) Filoti, G.; Kuźmin, M. D.; Bartolomé, J. *Phys. Rev. B* **2006**, *74*, 134420.
(47) Zhao, A.; Li, Q.; Chen, L.; Xiang, H.; Wang, W.; Pan, S.; Wang, B.; Xiao, X.; Yang, J.; Hou, J. G.; Zhu, Q. *Science* **2005**, *309*, 1542–4.
(48) Barlow, D. E.; Scudiero, L.; Hipps, K. W. *Langmuir* **2004**, *20*, 4413–21.
(49) Gavioli, L.; Fanetti, M.; Sancrotti, M.; Betti, M. G. *Phys. Rev. B* **2005**, *72*, 035458.
(50) Ferretti, A.; Baldacchini, C.; Calzolari, A.; Di Felice, R.; Ruini, A.; Molinari, E.; Betti, M. G. *Phys. Rev. Lett.* **2007**, *99*, 046802.
(51) Baldacchini, C.; Mariani, C.; Betti, M. G.; Vobornik, I.; Fujii, J.; Annese, E.; Rossi, G.; Ferretti, A.; Calzolari, A.; Di Felice, R.; Ruini, A.; Molinari, E. *Phys. Rev. B* **2007**, *76*, 245430.

JP108734U